# Triggering sleep slow waves by transcranial magnetic stimulation

**Marcello Massimini*†, Fabio Ferrarelli*, Steve K. Esser*, Brady A. Riedner*, Reto Huber*, Michael Murphy*, Michael J. Peterson*, and Giulio Tononi*‡**

*Department of Psychiatry, University of Wisconsin, 6001 Research Park Boulevard, Madison, WI 53719; and †Department of Clinical Sciences, University of Milan, Via G.B. Grassi 74, 20157 Milan, Italy

Communicated by Rodolfo R. Llinas, New York University Medical School, New York, NY, March 16, 2007 (received for review November 26, 2006)

**During much of sleep, cortical neurons undergo near-synchronous slow oscillation cycles in membrane potential, which give rise to the largest spontaneous waves observed in the normal electroencephalogram (EEG). Slow oscillations underlie characteristic features of the sleep EEG, such as slow waves and spindles. Here we show that, in sleeping subjects, slow waves and spindles can be triggered noninvasively and reliably by transcranial magnetic stimulation (TMS). With appropriate stimulation parameters, each TMS pulse at <1 Hz evokes an individual, high-amplitude slow wave that originates under the coil and spreads over the cortex. TMS triggering of slow waves reveals intrinsic bistability in thalamocortical networks during non-rapid eye movement sleep. Moreover, evoked slow waves lead to a deepening of sleep and to an increase in EEG slow-wave activity (0.5–4.5 Hz), which is thought to play a role in brain restoration and memory consolidation.**

consciousness | electroencephalogram | slow oscillation | bistability | perturbation

During non-rapid eye movement (NREM) sleep, the membrane potential of cortical neurons alternates between a depolarized up-state and a hyperpolarized down-state every second or so (1, 2). When these oscillations are near-synchronous and involve the majority of the cortex, they are readily visible in the electroencephalogram (EEG) as slow waves of large amplitude, often exceeding 100 $\mu$V, which constitute the largest electrical potential produced by the brain under normal conditions. Slow oscillations (SOs) originate locally and expand over the cortex as traveling waves that repeat several hundred times every night (3). The alternation of up- and down-states in cortical neurons is thought to be involved in memory consolidation (4, 5), synaptic homeostasis (6), and the restorative function of sleep (7, 8), so the ability to trigger slow waves reliably could have important applications.

During sleep, SO-like events (K-complexes) can indeed be evoked by auditory and other sensory stimuli (9, 10), but the triggering is sporadic and often accompanied by the subsequent suppression of endogenous slow waves and possible awakening. In animals, SOs have occasionally been elicited by direct electrical stimulation of the cortex under sleep-like anesthesia (11). We therefore asked whether it is possible to trigger slow waves noninvasively in humans by focally perturbing the sleeping cortex using transcranial magnetic stimulation (TMS).

## Results

**Each TMS Pulse Triggers a Slow Wave That Resembles a Spontaneous One.** We recorded the EEG response to TMS by means of a 60-channel TMS-compatible amplifier (12). At the beginning of the sleep period we applied TMS at different intensities and at various cortical sites to identify the optimal stimulation parameters for the triggering of slow waves. An MRI-guided navigation system was used to calculate in real time the strength and location of the electric field induced on the surface of the brain of six subjects (see *Methods*). Once optimal stimulation parameters had been identified, TMS was applied in blocks of 40 stimuli at ≈0.8 Hz (TMS-ON), separated by control periods of 1 min (TMS-OFF).

Fig. 1*A* shows a typical example of the results obtained after the site and intensity of the stimulation had been optimized: the very first TMS pulse in the TMS-ON sequence triggered a single slow wave of high amplitude (>80 $\mu$V), contrasting sharply with the lower amplitude waves of the preceding EEG; moreover, each of the following TMS pulses reliably triggered another slow wave with the same characteristics. In all subjects the EEG promptly returned to background level after cessation of the stimulation, indicating that no abnormal seizure-like activity had been induced. The spontaneous EEG pattern of light NREM sleep during TMS-OFF periods was replaced, during each TMS-ON period, by a pattern resembling the deepest NREM sleep as observed, for instance, during recovery from sleep deprivation (13). When the recordings were scored according to standard criteria (14) by investigators blind to the TMS procedure, TMS-ON periods were systematically classified as stage 4 sleep, whereas TMS-OFF epochs were mostly classified as stage 2.

We asked whether the slow waves evoked by TMS represent genuine sleep SOs. First, spontaneous SOs recorded from the scalp of humans are identified based on period-amplitude criteria (negative peak amplitude of at least 80 $\mu$V and half-wave duration between 0.125 and 1 s): TMS-evoked waves matched these criteria and had a similar shape (Fig. 1*B*). Second, as demonstrated by animal and human studies (15, 16), the up-state of the SO, corresponding to the surface-positive portion of the wave, can trigger and group thalamic spindles (a waxing–waning oscillation at ≈12–15 Hz): similarly, the positive portion of the TMS-evoked wave was associated with a significant increase in spindle amplitude (Fig. 1*C*). Third, spontaneous sleep slow waves behave as traveling waves that spread smoothly over wide regions of the scalp (3): the negative peak of the waves triggered by TMS displayed a topographic delay gradient similar to the one of spontaneous slow waves (Fig. 1*D*). In summary, each TMS pulse triggered an individual slow wave that, like spontaneous sleep slow waves, had high amplitude and long duration, entrained thalamic spindles, and spread over the scalp. However, unlike spontaneous SOs, which can originate at many different sites over the cortical surface, TMS-induced slow waves predictably originated in a restricted area under the stimulating coil (Fig. 1*E*). Unlike K-complexes (SOs that are sporadically induced by peripheral stimuli and are gated by subcortical mechanisms), TMS-evoked slow waves, being produced by direct

Author contributions: M. Massimini and G.T. designed research; M. Massimini, F.F., S.K.E., B.A.R., R.H., M. Murphy, and M.J.P. performed research; M. Massimini and F.F. analyzed data; and M. Massimini and G.T. wrote the paper.

The authors declare no conflict of interest.

Abbreviations: TMS, transcranial magnetic stimulation; NREM, non-rapid eye movement; EEG, electroencephalogram; SWA, slow-wave activity; SO, slow oscillation.

‡To whom correspondence should be addressed. E-mail: gtononi@wisc.edu.

This article contains supporting information online at www.pnas.org/cgi/content/full/0702495104/DC1.

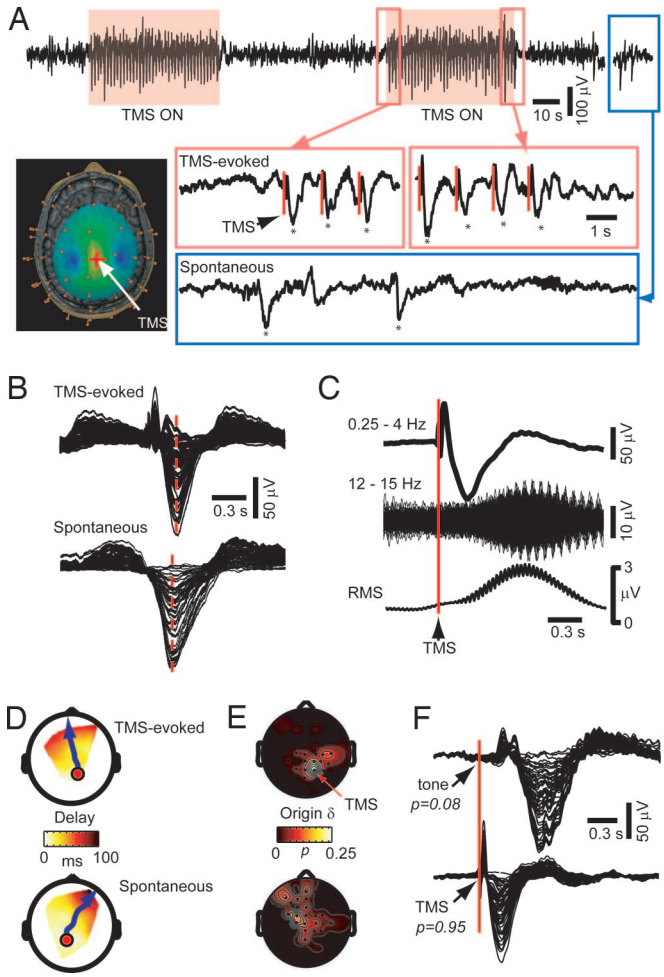


**Fig. 1.** TMS during sleep triggers slow waves that resemble spontaneously occurring ones. (*A Upper*) The signal recorded from a channel (Cz) located under the stimulator during two TMS-ON blocks over a background of spontaneous NREM sleep (single-subject data). Each TMS-ON block consisted of 40 stimuli at ≈0.8 Hz. The stimulation site (hot spot) is marked by a red cross on the cortical surface. The red highlighted sections show the slow waves triggered at the beginning and at the end of one block. Spontaneously occurring slow waves recorded from the same subject a few minutes later are depicted in the blue highlighted section. (*B*) TMS-evoked and spontaneous slow waves, recorded from all channels, were detected based on period-amplitude criteria and averaged on the negative peak. TMS-evoked and spontaneous slow waves had similar shape. (*C*) The average signal recorded from Cz was band-pass filtered (0.25–4 Hz) in the top trace. In the middle and bottom traces the corresponding single trials were filtered in the spindles frequency range (12–15 Hz) and rectified (rms). The positive wave of the TMS-evoked slow wave was associated with an increase in spindle amplitude. (*D*) The delay gradient of the negative peak is shown for a single TMS-evoked slow wave (*Upper*) and for a single spontaneous slow wave (*Lower*). The red dot marks the location of the channel with delay = 0 (origin). The blue lines starting from the origin represent the streamlines calculated on the vector field of delays. TMS-evoked slow waves, like spontaneous ones, spread on the scalp as traveling waves. (*E*) The probability of each electrode being the origin of a traveling wave is shown for both TMS-evoked and spontaneous slow waves. TMS-evoked slow waves originated more frequently from the area underlying the stimulator. (*F*) TMS-evoked slow waves and auditory evoked K-complexes, recorded from all channels, were detected based on period-amplitude criteria and averaged. The value indicates the probability of evoking a slow wave with TMS and auditory stimulation at 0.8 Hz. Unlike TMS, auditory stimuli triggered slow waves unreliably and with an ≈300-ms delay.

cortical stimulation, had much shorter latencies (≈300 ms less) (Fig. 1*F*) and could be evoked reliably by each and every stimulus (triggering probability: 0.95).

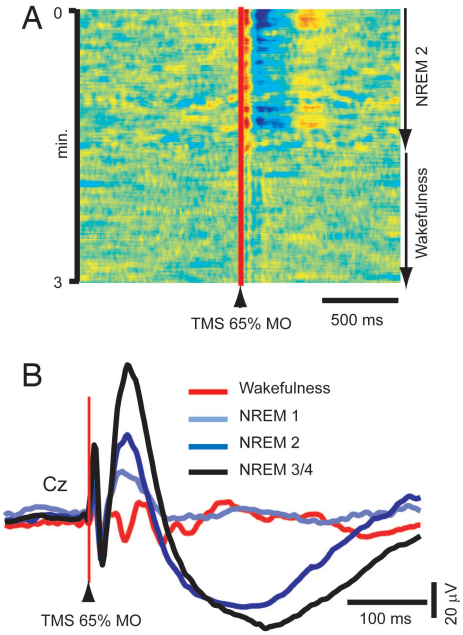


**Fig. 2.** TMS triggering of slow waves is state-specific. (*A*) TMS-evoked single-trial responses during a transition from NREM sleep to wakefulness. MO, maximal stimulator output. Voltage is color-coded (red, positive; blue, negative). During NREM sleep, each TMS pulse triggered a slow wave (prominent negative deflection followed by a positive rebound). Awakening was associated with the sudden disappearance of the slow wave response, which was replaced by low-amplitude, fast-frequency components. (*B*) Average TMS-evoked potential recorded from Cz during different states of vigilance in a single subject. TMS evoked slow waves resembling high-amplitude spontaneous slow waves only during sleep stages 2, 3, and 4.

**TMS Triggering of Slow Waves Is State-Dependent.** Regardless of stimulation site and intensity, TMS pulses that evoked slow waves during NREM could not do so during wakefulness. Fig. 2*A* shows single-trial responses recorded from one channel (Cz) during a transition from NREM sleep to wakefulness. During sleep, the initial activations evolved into the large negative–positive sequence characteristic of the SO. Shortly before overt EEG awakening, the large negative wave disappeared. As shown in Fig. 2*B*, the full-blown negative wave was present in NREM stages 2, 3, and 4, was much reduced during the transitional stage 1, and disappeared completely during wakefulness.

**TMS Triggering of Slow Waves Is Dose- and Site-Dependent.** As shown in Fig. 3, we systematically probed the ability of TMS to evoke a slow wave by stimulating, at four increasing intensities, four midline cortical sites along the posterior–anterior axis. In all subjects, full-blown SOs could be elicited reliably when stimulating the scalp area overlying sensorimotor cortex. Posterior parietal sites were less effective, and anterior sites, such as rostral premotor cortex, were least effective. However, we could not probe orbitofrontal, temporal, and occipital sites without causing scalp muscle activation. The intensity required to trigger full-fledged slow waves over sensorimotor cortex varied across subjects between 65% and 85% of maximal stimulator output, corresponding to a maximal electric field of 150–180 V/m on the cortical surface; lower intensities proved less effective or ineffective. The intensity of the field (calculated based on distance from the scalp) did not differ appreciably between effective and less effective regions (data not shown). The triggering of slow waves could be obtained reliably also at frequencies <0.8 Hz; frequencies >1 Hz were not explored.

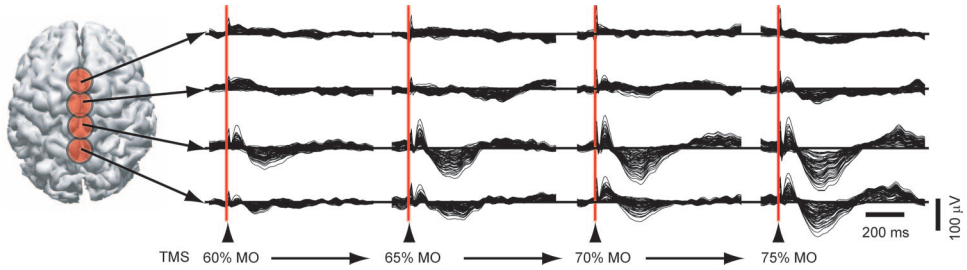


**Fig. 3.** TMS triggering of slow waves is dose- and site-dependent. TMS was delivered at four midline sites along the posterior–anterior axis of the cortex (posterior parietal, sensorimotor, supplementary motor, and rostral premotor). The brain response to TMS was probed, at each site, at four increasing intensities (MO, maximum stimulator output). The average responses to 15 TMS trials recorded from all channels (referenced to the mastoid) is shown for each intensity and each cortical site (the data refer to an individual subject). The amplitude of the negative peak depended on stimulation intensity. However, the ability of TMS to trigger slow waves changed markedly along the posterior–anterior axis: High-amplitude slow waves could be elicited reliably only when stimulating sensorimotor cortex, whereas stimulation of more anterior cortical sites produced low-amplitude waves.

**TMS Triggers Local, or Global, Slow Waves During Sleep and a Differentiated Response During Wakefulness.** Fig. 4 *A*–*C* and *A′*–*C′* show the averaged traces, the scalp potentials, and the cortical currents induced by TMS delivered in two different cortical areas during NREM sleep. A lateral stimulation site, corresponding to dorsal premotor cortex, is compared with the triggering hot spot overlying sensorimotor cortex. Note how the anterior stimulation site produced a prominent positive component, followed by a small negative wave (Fig. 4*A*); cortical currents remained local until they dissipated gradually (Fig. 4 *B* and *C*). The sensorimotor stimulation site produced initially a similar response, but this was soon followed by a large-amplitude negative wave (Fig. 4*A′*). The current maps, obtained by using a realistic head model and L2 Norm, shows a maximum at the stimulation site, which soon spread broadly over the surrounding cortex in an oil-spot manner (Fig. 4 *B′* and *C′*). During wakefulness TMS, delivered at the same intensity and target, evoked instead a low-amplitude, complex wave shape that was associated with a differentiated pattern of long-range cortical activation (Fig. 4 *A″*–*C″*) (17).

**TMS Triggering of Slow Waves Leads to a Marked Increase of Slow-Wave Activity (SWA).** SOs are thought to underlie EEG SWA (0.5–4.5 Hz) (18), a reliable indicator of sleep need that is thought to mediate the restorative function of NREM sleep (6, 8). We therefore asked whether the repeated induction of individual slow waves by each TMS pulse would lead to an increase in sleep SWA. Using a block design protocol (all-night stimulation was not easily feasible with the present setup), we examined the time course of mean SWA power recorded from all electrodes during the alternation of TMS-ON and TMS-OFF blocks (Fig. 5*A*). We also investigated associated changes in topography (Fig. 5*B*) and spectral profile (Fig. 5*C*). Fig. 5 *D* and *E* shows individual results for each subject. When applied to sensorimotor cortex with an interstimulus interval between 1.1 and 1.3 s, TMS led to an increase in SWA power of up to eight times around the stimulation site and to a 2-fold increase over the rest of the scalp. Control experiments using TMS blocks at ineffective sites as well as supramaximal stimulation of sensorimotor nerves produced no changes in SWA [see supporting information (SI) *Text* and SI Fig. 6], indicating that the observed effects were not due to peripheral factors. Importantly, the power increase was not limited to the stimulation frequency, but was significant ($P < 0.01$) in the entire SWA frequency band (Fig. 5*C*). Manipulations affecting sleep homeostasis, for example, sleep deprivation, produce a similar spectral profile (19).

## Discussion

Sleep slow waves and K-complexes represent the largest physiological EEG signal produced by the brain and correspond to the fundamental electrical phenomenon underlying NREM sleep. We show here that, using TMS, it is possible to trigger reliably slow waves in humans that resemble in all aspects spontaneously occurring slow waves and K-complexes. Similar to a cardiac pacemaker, each and every TMS pulse, delivered during NREM sleep, triggered a slow wave that started under the stimulator and spread like an oil spot to the rest of the brain. TMS triggering of slow waves was dose- and site-dependent and led to a marked increase of SWA over the scalp.

Animal recordings show that the negative phase of the SOs is associated with hyperpolarization and cessation of firing (down-state) throughout the cortex (20). Thus, it is likely that the negative component of the slow wave triggered by sensorimotor TMS is associated with a long-lasting period (hundreds of milliseconds) of neuronal silence in vast regions of the brain (see *SI Text* and SI Fig. 7). As indicated by computer simulations (21–23) and *in vitro* recordings (24), the occurrence of SOs during NREM sleep reflects an intrinsic bistability of thalamocortical networks between up- and down-states that is brought about by neuromodulatory changes (25). TMS over the sensorimotor cortex could trigger a slow wave at any time during NREM sleep, including stage-2 epochs when the ongoing EEG showed little spontaneous fluctuations (Fig. 1*A*). Thus, TMS pulses reveal the fundamental bistability of the sleeping cortex. Indeed, whereas during sleep TMS pulses always triggered a stereotyped down-state, either local or global (Fig. 4 *A*–*C* and *A′*–*C′*), long-range, spatially, and temporally differentiated responses to TMS were obtained only when the subjects were awake (Fig. 4 *A″*–*C″*). These findings suggest that the sleeping brain, despite being active and reactive, loses its ability of entering states that are both integrated and differentiated: it either breaks down in independent modules (producing a local slow wave) or bursts into an explosive and aspecific response (producing a global slow wave). Both features may be important to account for the fading of consciousness during the early phase of sleep (26).

At this stage we can only speculate on why sensorimotor regions constitute a preferential site for triggering with TMS waves that resemble full-fledged SOs. The hot spot for TMS-triggered SOs corresponds closely to a hot spot for the origin of spontaneous slow waves (3). There are other prominent hot spots for spontaneous slow waves over orbitofrontal cortex, but those could not be probed by TMS without causing discomfort and awakening the subjects. Sensorimotor cortex is also the brain region where EEG recordings show the maximum density of vertex sharp waves (27) and spindle oscillations (28). Because sleep spindles are generated by the reticular thalamic nucleus and its interactions with the thalamus, it is possible that a strong activation of corticoreticulothalamocortical circuits by TMS may help the induction of SOs. Low-frequency bursting of hyperpolarized thalamic neurons (29) may also reduce inhibitory sculp-

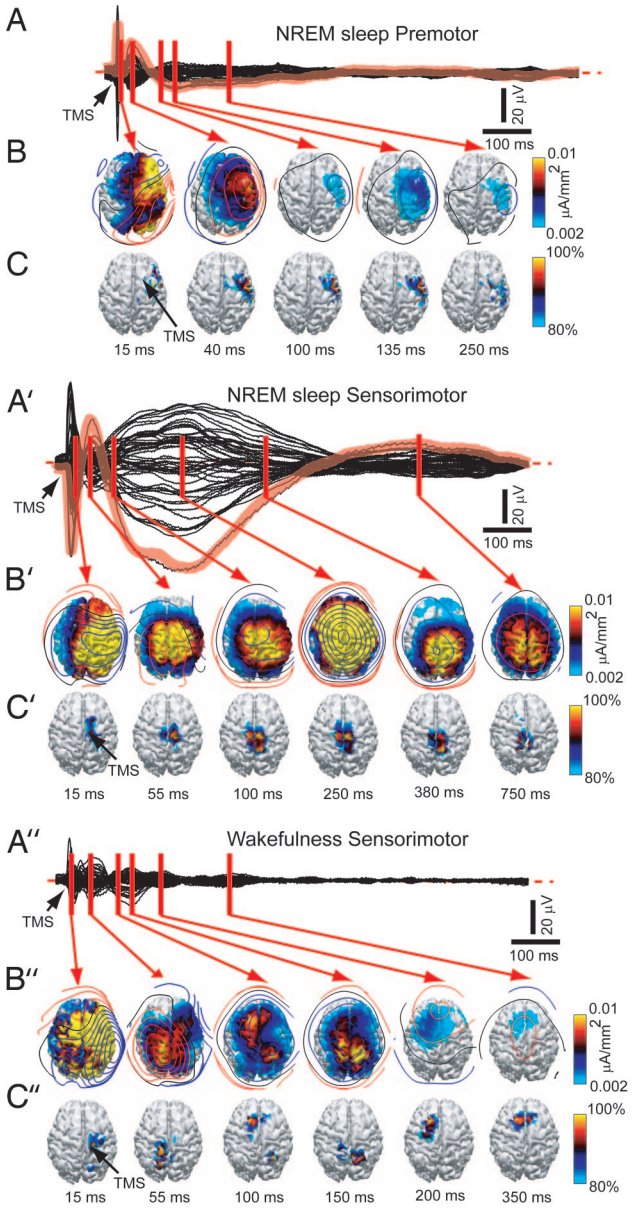


**Fig. 4.** Cortical activation evoked by TMS. (*A* and *A′*) Averaged TMS-evoked potentials recorded at all electrodes, superimposed in a butterfly diagram for a low-amplitude wave triggered from premotor cortex (top) and for a high-amplitude wave triggered from sensorimotor cortex (bottom) during sleep. The channel located under the stimulator is plotted in red. (*B* and *B′*) The absolute current density in the cerebral cortex is estimated with L2 Norm at different time points and plotted together with the corresponding scalp voltage distribution (red, positive; blue, negative). (*C* and *C′*) The current density distribution is autoscaled and thresholded at 80% to highlight the location of maximum current sources. Whereas premotor stimulation gave rise to cortical currents that remained local, TMS in sensorimotor cortex triggered a large negative deflection associated with long-lasting currents that spread broadly to the surrounding cortex starting from a fixed local maximum. (*A″*–*C″*) TMS delivered over sensorimotor cortex during wakefulness evoked a low-amplitude, complex wave shape associated with a spatially and temporally differentiated pattern of activation. Maximum cortical activation shifted over time among distant cortical areas giving rise to a long-range, specific response.

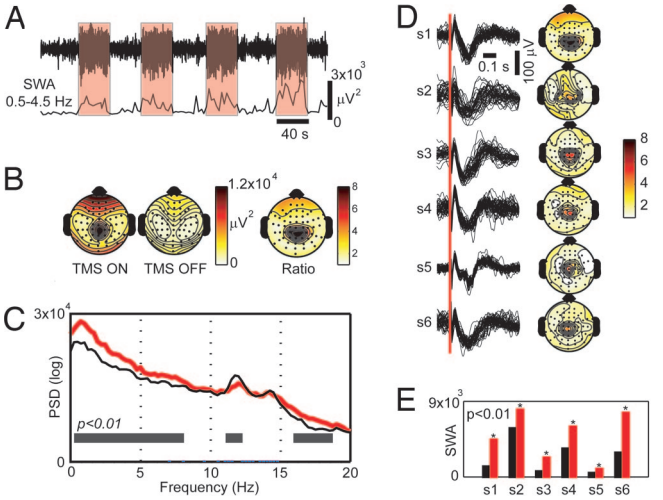


**Fig. 5.** The triggering of slow waves by each TMS pulse led to a marked increase of SWA. (*A*) The signal recorded from a channel under the stimulator (upper trace) and the time course of SWA power (0.5–4.5 Hz, 4-s windows, average of all sensors) are depicted during a complete block design sequence for an individual subject. (*B*) The topography of SWA during the TMS-ON block and during the TMS-OFF block, and their ratio. (*C*) Spectral profiles (average of all sensors) recorded during the TMS-ON blocks (red) and the TMS-OFF blocks (black). The gray horizontal bars indicate the significant bins ($P < 0.01$). (*D*) Summary of individual data: single responses to TMS, recorded from a channel (Cz) during the block design, are plotted (*Left*) together with the topography of the increase in SWA induced by TMS. (*E*) Shown for each subject is the average SWA power recorded from all sensors during TMS-OFF (black bars) and TMS-ON (red bars) blocks.

turing of cortical activity and facilitate the emergence of a large and aspecific response (30).

The reliable triggering of slow waves with each and every TMS pulse resulted in a substantial increase in SWA both locally (up to eight times) and globally (two times) over the scalp. TMS-evoked slow waves and enhancement of SWA could be obtained during all stages of NREM sleep (stages 2, 3, and 4), yet the most dramatic effect was observed when TMS was applied during stage 2. In this case, the repetitive triggering of individual slow waves produced a sudden electrophysiological transition to stage 4 (Fig. 1*A*).

The SO is the most fundamental cellular event underlying sleep EEG activity. Indeed, although born and discovered in the neocortex, the SO has been found to entrain the thalamus and, more recently, the basal ganglia, the paleocortex, and the hippocampus. Through its ability to group SWA, thalamic spindles, and hippocampal ripples (high-frequency oscillations associated with hippocampal sharp waves), the SO is thought to support memory consolidation during sleep (31). By imposing a repeating, low-frequency alternation of active and silent periods in cortical circuits, SOs may carry out the homeostatic control of synaptic weight (6). More generally, SWA is considered a reliable indicator of sleep need that increases with time awake, decreases during sleep (7), and may mediate the restorative function of slow-wave sleep (6, 8). Indeed, SWA is linked to the induction of cortical plastic changes, because it increases locally after a learning task and is positively correlated with post-sleep performance improvement (32). Recently, transcranial direct current stimulation during sleep at the frequency of the SO was reported to enhance declarative memory, although in that study brain activity could not be recorded during stimulation (33). By demonstrating that TMS pulses can trigger full-fledged SOs and enhance sleep SWA, locally and globally, the present study proves that endogenous sleep rhythms can be potentiated non-invasively and nonpharmacologically. Conceivable practical applications include enhancing the restorative value of short periods of sleep under conditions of sleep restriction (power naps) and the amelioration of negative symptoms associated with

NEUROSCIENCE

insomnia, aging, and psychiatric/neurological disorders characterized by disturbed sleep.

## Methods

**Subjects.** Fifteen male subjects (age 21–36) participated in the study. All participants gave written informed consent, and the experiment was approved by the University of Wisconsin Human Subjects Committee. Before the experiment a neurological screening was performed to exclude potential adverse effects of TMS. TMS was performed in accordance with current safety guidelines (34). The data presented here are from the six subjects in whom at least one full block design sequence of TMS (40 × 4 pulses) was carried out during NREM sleep. The remaining subjects either were not able to sleep or provided EEG data that were excessively contaminated by artifacts.

**TMS Targeting.** Stimulation was performed by means of a figure-of-eight coil (model P/N9925; Magstim, Whitland, U.K.), with a wing diameter of 70 mm, connected to a Magstim Rapid biphasic stimulator. Cortical TMS targets were identified on T1 weighted MRIs (resolution 0.5 mm) acquired with a 3T GE Signa scanner. To ensure precision and reproducibility of stimulation we used a Brain Navigated Stimulation (NBS) system (Nexstim, Helsinki, Finland). The NBS device located (with an error $< 3$ mm) the relative positions of the subject's head and of the TMS coil by means of an optical tracking system. NBS also calculated the distribution and the strength of the intracranial electric field induced by TMS. In this way, the exact location of the maximum electric field on the cortical surface (hot spot) could be monitored in real time. The coordinates of stimulation were input to a software aiming tool that ensured throughout the session the reproducibility of position, direction, and angle of the stimulator.

**EEG Recordings During TMS.** We recorded the spontaneous and TMS-evoked EEG by means of a 60-electrode cap and a specifically designed TMS-compatible amplifier (Nexstim). The artifact induced by TMS was gated, and saturation of the amplifier was avoided by means of a proprietary sample-and-hold circuit that kept the analog output of the amplifier constant from 100 $\mu$s before stimulus to 2 ms after stimulus (12). To further optimize TMS compatibility, the impedance at all electrodes was kept below 3 K$\Omega$. The EEG signals, referenced to an additional electrode on the forehead, were filtered (0.1–500 Hz) and sampled at 1,450 Hz with 16-bit resolution. Two extra sensors were used to record the electrooculogram. In most cases no signs of TMS-induced magnetic artifact were detected, and in all cases the EEG signals were artifact-free from $<$10 ms after stimulus.

**Masking of the TMS Click.** The click associated with the coil's discharge propagates through air and bone and can elicit an auditory N1-P2 complex at latencies of 100–200 ms (35). Moreover, during NREM sleep, auditory stimulation may sporadically evoke a K-complex (9). To prevent contamination of TMS-evoked potentials as well as interference with spontaneous sleep EEG patterns, a procedure was adopted to completely eliminate the subject's perception of the coil's click. The waveform of the TMS click was digitized and processed to produce a continuous audio signal that captures its specific time-varying frequencies. Before the experiment, we delivered regular TMS test pulses (at intensities increasing up to 80% maximum stimulator output) to the subjects while the masking noise was played through inserted earplugs. At this time we adjusted the masking volume (always $<$90 dB) until the subjects reported that the TMS click was not perceptible. Bone conduction was attenuated by placing a thin layer of foam between the coil and the EEG cap. These procedures have previously been shown to effectively abolish the auditory stimulation associated with TMS (17).

**General Experimental Procedures.** During the experiment each subject was lying with eyes closed on a reclining chair with a head-rest that allowed a comfortable and stable head position. Noise masking was played throughout the recording session. After preparation for EEG recordings and calibration of the navigation system the subject was allowed to fall asleep. After subjects entered a consolidated period ($>$5 min) of NREM sleep stage 2, we started probing for the triggering of slow waves at various cortical sites and at increasing intensities. In all subjects we stimulated four midline cortical sites along the posterior–anterior axis (posterior parietal, sensorimotor, supplementary motor, and rostral premotor). At each site we first delivered series of 15 pulses (at a frequency of 0.5 Hz) at 60% maximal output. If this first series did not produce a manifest slow wave triggering on the ongoing EEG, stimulation intensity was increased by 5% and another series of 15 pulses was delivered. This procedure was repeated until waves resembling full-blown SOs were reliably evoked or until a maximum intensity of 85% was reached. In addition to the four midline targets, in most of the subjects we also probed sites located 2–3 cm lateral to the midline in both hemispheres.

In each subject the site at which full-blown SOs could be elicited at the lowest intensity was selected for the block design protocol. The protocol consisted of four blocks of stimuli at $\approx$0.8 Hz (TMS-ON) separated by control periods of 1 min (TMS-OFF). Longer block design or all-night stimulations were not possible because of coil overheating and because of the fact that, to ensure a stable coil positioning, the subject had to sleep on a reclining chair. In four subjects the spontaneous EEG showed a pattern of NREM sleep stage 2 throughout the TMS-OFF periods whereas in two subjects some epochs of stage 3 were scored during the last two TMS-OFF periods of the block design.

Once the block design was successfully completed, we recorded the ongoing sleep EEG to collect a representative number of spontaneous SOs. In addition, in some subjects ($n$ = 3) we delivered various blocks of auditory tones, at different frequencies from 0.1 Hz to 0.8 Hz, to evaluate the rate of occurrence and the wave form of auditory evoked K-complexes.

**Data Analysis.** Data analysis was performed by using Matlab (The MathWorks, Natick, MA), the public license toolbox EEGLAB (36), and Curry 5.0 (Philips, Cologne, Germany). TMS trials containing noise, muscle activity, or eye movements were rejected. For the comparison between TMS-evoked SOs, spontaneous SOs, and auditory evoked K-complexes the EEG signals were referenced to the mathematically linked mastoids. The criteria for the detection of TMS-evoked SOs were the same as those previously used to detect spontaneous SOs (3): (*i*) a negative zero-crossing and a subsequent positive zero-crossing separated by 0.3–1 s and (*ii*) a negative peak between the two zero-crossings with voltage $<$80 $\mu$V. To evaluate the ability of TMS-evoked SOs to group spindle activity, single SOs triggered by TMS and recorded from Cz were filtered in the spindle frequency range (12–15 Hz). After subtraction of the mean, the rms of the filtered signal was calculated and averaged as in ref. 16. To study the traveling of spontaneous and TMS-evoked SOs we calculated delay maps of the negative peak as in ref. 3. For each cycle, the delay of the negative peak was studied topographically. The delay values measured at each electrode's location were transposed into Cartesian coordinates space (Fig. 1*D*). To avoid any interpolation of the measured data we used a low-resolution grid (50 × 50). The delay map condensed the information relative to the spatial distribution and the timing of a SO on the scalp. The minimum value of the delay map, corresponding to the coordinates of the first electrode that recorded the negative peak, was defined as the origin of the cycle. To evaluate the continuity and the main direction of the gradient of delays that surrounded the origin we used the

streamlines (blue lines in Fig. 1*D*). Each streamline is tangential to the instantaneous velocity direction and progresses in the 2D vector field of delays until the gradient is broken. The origin density map, displayed in Fig. 1*E*, is obtained by interpolating the probability of each electrode to be the origin of the SO. This map highlights the scalp foci where SOs are more likely to originate and allows for direct comparison among conditions.

For source modeling and spectral analysis the EEG signal was referenced to the average of all electrodes. Source modeling was performed by using a realistic head model derived from individual MRIs. The averaged responses, the MRI sets, and the electrode coordinates were input to the software package Curry 5.0. As a first step we performed noise estimation by calculating the variance of the data in a 300-ms prestimulus window. In all cases the average noise level was below 1 $\mu$V (range: 0.3–0.7 $\mu$V). The results of noise estimation were subsequently used to determine the sensor weighting and the regularization parameter ($\lambda$) of the current density reconstruction. After a semiautomatic segmentation of the individual MRIs we implemented a boundary element model of the head having three compartments of fixed conductivities (scalp, 0.33 S/m; skull, 0.0042 S/m; brain, 0.33 S/m). The cortical surface was also reconstructed with a 6-mm resolution and modeled with $\approx$14,000 rotating dipoles. Next, the electrode positions were projected onto the skin surface and the lead field matrix was calculated. We estimated the current density on the cortical surface using the minimum norm least squares method (L2 Norm, weighted for depth bias removal). The L2 Norm has the advantage of requiring no *a priori* assumption about the nature of the source distribution (37) and of providing stable solutions also in the presence of noise (38). Although this method results in a blurred picture of cortical activation, the location of the maximum estimated current reflects with good accuracy ($<$10 mm) the location of the center of neural activity (39). A detailed description of the assumptions and methods used for MRI processing and source reconstruction can be found elsewhere (40, 41). Cortical activations were plotted both in absolute and relative scale to compare the strength and spatial extent of evoked currents as well as the location of maximal neural activity in the different conditions. For spectral analysis the EEG recordings were down-sampled at 500 Hz and band-pass filtered between 0.5 Hz and 40 Hz. Spectral analysis (FFT routine, Hanning window, averages of five 4-s epochs) was performed for all 60 channels. Spectral power was averaged at all sensors, the time course of SWA (0.25–0.45 Hz) was calculated, and a two-tailed *t* test was used to evaluate the changes in SWA associated with the TMS-OFF and the TMS-ON blocks.

We thank Andy Alexander, Chiara Cirelli, Ruth Benca, and Florinda Ferreri for their help and comments. This work was supported by a National Institutes of Health Pioneer Award (to G.T.).

1. Steriade M, Nunez A, Amzica F (1993) *J Neurosci* 13:3252–3265.
2. Steriade M, Timofeev I, Grenier F (2001) *J Neurophysiol* 85:1969–1985.
3. Massimini M, Huber R, Ferrarelli F, Hill S, Tononi G (2004) *J Neurosci* 24:6862–6870.
4. Sejnowski TJ, Destexhe A (2000) *Brain Res* 886:208–223.
5. Steriade M, Timofeev I (2003) *Neuron* 37:563–576.
6. Tononi G, Cirelli C (2006) *Sleep Med Rev* 10:49–62.
7. Borbely A, Achermann P (2005) in *Principles and Practice of Sleep Medicine*, eds Kryger MH, Roth T, Dement WC (Saunders, Philadelphia), pp 405–418.
8. Walsh JK, Randazzo AC, Stone K, Eisenstein R, Feren SD, Kajy S, Dickey P, Roehrs T, Roth T, Schweitzer PK (2006) *Sleep* 29:433–443.
9. Bastien C, Campbell K (1992) *Sleep* 15:236–245.
10. Niiyama Y, Satoh N, Kutsuzawa O, Hishikawa Y (1996) *Electroencephalogr Clin Neurophysiol* 98:394–400.
11. Amzica F, Steriade M (1998) *Neuroscience* 82:671–686.
12. Virtanen J, Ruohonen J, Naatanen R, Ilmoniemi RJ (1999) *Med Biol Eng Comput* 37:322–326.
13. Feinberg I, Floyd TC, March JD (1987) *Electroencephalogr Clin Neurophysiol* 67:217–221.
14. Retchtshafflen A, Kales A (1968) *A Manual of Standardized Terminology, Techniques and Scoring System for Sleep Stages of Human Subjects* (Natl Inst of Health, Washington, DC).
15. Steriade M, Contreras D, Curro Dossi R, Nunez A (1993) *J Neurosci* 13:3284–3299.
16. Molle M, Marshall L, Gais S, Born J (2002) *J Neurosci* 22:10941–10947.
17. Massimini M, Ferrarelli F, Huber R, Esser SK, Singh H, Tononi G (2005) *Science* 309:2228–2232.
18. Steriade M (2003) *Front Biosci* 8:d878–d899.
19. Achermann P, Finelli LA, Borbely AA (2001) *Brain Res* 913:220–223.
20. Destexhe A, Contreras D, Steriade M (1999) *J Neurosci* 19:4595–4608.
21. Bazhenov M, Timofeev I, Steriade M, Sejnowski TJ (2002) *J Neurosci* 22:8691–8704.
22. Compte A, Sanchez-Vives MV, McCormick DA, Wang XJ (2003) *J Neurophysiol* 89:2707–2725.
23. Hill S, Tononi G (2005) *J Neurophysiol* 93:1671–1698.
24. Sanchez-Vives MV, McCormick DA (2000) *Nat Neurosci* 3:1027–1034.
25. Steriade M (2004) *Prog Brain Res* 145:179–196.
26. Tononi G (2004) *BMC Neurosci* 5:42.
27. Colrain IM, Webster KE, Hirst G, Campbell KB (2000) *Sleep* 23:97–106.
28. Finelli LA, Borbely AA, Achermann P (2001) *Eur J Neurosci* 13:2282–2290.
29. Llinas RR, Steriade M (2006) *J Neurophysiol* 95:3297–3308.
30. Llinas R, Urbano FJ, Leznik E, Ramirez RR, van Marle HJ (2005) *Trends Neurosci* 28:325–333.
31. Molle M, Yeshenko O, Marshall L, Sara SJ, Born J (2006) *J Neurophysiol* 96:62–70.
32. Huber R, Ghilardi MF, Massimini M, Tononi G (2004) *Nature* 430:78–81.
33. Marshall L, Helgadottir H, Molle M, Born J (2006) *Nature* 444:610–613.
34. Wassermann EM (1998) *Electroencephalogr Clin Neurophysiol* 108:1–16.
35. Nikouline V, Ruohonen J, Ilmoniemi RJ (1999) *Clin Neurophysiol* 110:1325–1328.
36. Delorme A, Makeig S (2004) *J Neurosci Methods* 134:9–21.
37. Hamalainen MS, Ilmoniemi RJ (1994) *Med Biol Eng Comput* 32:35–42.
38. Silva C, Maltez JC, Trindade E, Arriaga A, Ducla-Soares E (2004) *Clin Neurophysiol* 115:1657–1668.
39. Hauk O (2004) *NeuroImage* 21:1612–1621.
40. Buchner H, Knoll G, Fuchs M, Rienacker A, Beckmann R, Wagner M, Silny J, Pesch J (1997) *Electroencephalogr Clin Neurophysiol* 102:267–278.
41. Fuchs M, Wagner M, Kohler T, Wischmann HA (1999) *J Clin Neurophysiol* 16:267–295.